Journal of Complex Networks (2017) **5**, 712–733
doi: 10.1093/comnet/cnx003
Advance Access Publication on 15 May 2017

Contact process with exogenous infection and the scaled SIS process

JUNE ZHANG† AND JOSÉ M.F. MOURA
Department of Electrical and Computer Engineering, Carnegie Mellon University, Pittsburgh, PA 15213, USA
†Corresponding author. Email: junez@andrew.cmu.edu

AND

JUNE ZHANG
Department of Electrical Engineering, University of Hawai'i at Manoa, Honolulu, HI 96822, USA

Edited by: Matt Keeling

[Received on 5 June 2015; editorial decision on 16 February 2017; accepted on 3 May 2017]

Propagation of contagion in networks depends on the graph topology. This article is concerned with studying the time-asymptotic behaviour of the extended contact processes on static, undirected, finite-size networks. This is a contact process with nonzero exogenous infection rate (also known as the ϵ-susceptible-infected-susceptible model). The only known analytical characterization of the equilibrium distribution of this process is for complete networks. For large networks with arbitrary topology, it is infeasible to numerically solve for the equilibrium distribution since it requires solving the eigenvalue-eigenvector problem of a matrix that is exponential in N, the size of the network. We derive a condition on the infection rates under which, depending on the degree distribution of the network, the equilibrium distribution of extended contact processes on *arbitrary*, finite-size networks is well approximated by a closed-form formulation. We confirm the goodness of the approximation with small networks answering inference questions like the distribution of the percentage of infected individuals and the most-probable equilibrium configuration. We then use the approximation to analyse the equilibrium distribution of the extended contact process on the 4941-node US Western power grid.

Keywords: scaled SIS process, contact process; ϵ-SIS; epidemics on networks; network science; network process.

1. Introduction

Classic epidemics models assume homogeneous mixing, where each infected individual has the same number of contacts with susceptible individuals; the infection rate due to contagion is assumed to be dependent on some fraction of the total number of infected and susceptible individuals in the population. Realistically, however, individuals are not homogenous as some individuals are more connected than others. Newer models such as structured population models try to account for distinguishing individual characteristics such as age, location, infectivity, interactions, etc. [2]. Network-based epidemics models incorporate the contact networks, which describe heterogenous interactions between individuals in a given population, as a determinant of the observed dynamics [3–6].

In this paper, we are interested in understanding the effect of the contact network on the time-asymptotic behaviours of the ϵ-SIS (susceptible-infected-susceptible) model [1]. The ϵ-SIS (susceptible-infected-susceptible) model is an extension of the contact process introduced in [7] by assuming a nonzero exogenous (i.e., spontaneous) infection rate. We will refer to the ϵ-SIS (susceptible-infected-susceptible) model as the extended contact process in this paper. In addition to a nonzero exogenous infection rate, the extended contact process also assumes that the infection rate of a susceptible agent is linearly dependent on the number of contacts with infected individuals (i.e., the number of infected neighbours in the contact network), thereby explicitly coupling the underlying contact network to the dynamics.

Due to the inclusion of a nonzero exogenous infection rate, the extended contact process does not have a trivial equilibrium distribution. Computing the equilibrium distribution of a finite-length Markov process, such as the extended contact process, requires solving an eigenvalue-eigenvector problem. As the number of Markov states is exponential in the size of the network, it is an infeasible computation problem to solve for the equilibrium distribution of the extended contact process parameterized by networks with hundreds or thousands of individuals. When dealing with large-scale networks, researchers usually approximate them with infinite-size networks using the mean-field approximation [1]. We take a different approach and show that, for a subclass of extended contact processes, their equilibrium distribution can be approximated by that of the scaled SIS process, for which we found the closed-form equilibrium distribution of the process on *arbitrary*, undirected, finite-size network topology [8, 9]. Unlike the extended contact process, which assumes that the infection rate of a healthy agent is linearly dependent on its number of infected neighbours, the scaled SIS process assumes an exponential dependence.

When the infection rates of the scaled SIS process are appropriately scaled to equal the rates of the extended contact process, we can describe the equilibrium behaviour of the extended contact process for arbitrary networks with thousands of individuals *without* any further approximation. The closed-form equilibrium distribution of the extended contact process informs us that its equilibrium behaviour depends on (1) individual susceptibility to be in healthy vs. infected state (i.e., the ratio of the exogenous infection rate over the healing rate) and (2) the effective contribution of contagion vs. spontaneous infection (i.e., the ratio of the endogenous infection rate over the exogenous infection rate). With a known equilibrium distribution, we can answer inference questions such as what is the distribution of the percentage of infected individuals or what is the most-probable configuration, the configuration with maximum equilibrium probability. The former informs us of the vulnerability of the entire population, and the latter can help us identify which agents and network substructures are more susceptible to infection.

We review the extended contact process in Section 2.1, the scaled SIS process in Section 2.2. We compare and contrast the two network processes in Section 2.3. In Section 3, we derive a condition, depending on the degree distribution of the network, under which the equilibrium distribution of the extended contact process is well approximated by that of the scaled SIS process. In Section 4, we compare the true equilibrium distribution of the extended contact process with its approximation for six different 16-node networks using total variation distance. The small size of these networks ensures that we can compute the true equilibrium distribution of the extended contact process. These studies confirm the goodness of the approximation. We discuss the most-probable configuration of the extended contact process and the approximate distribution in Section 5. We then use our approximation to study the extended contact process in a much larger network for which it is infeasible to resort to numerical method. This is carried out in Section 6 where we examine the equilibrium behaviour of the extended contact process on the 4941-node US Western power grid. Section 7 concludes the paper.

2. Contact process and scaled SIS process

The contact process models the spread of infection in a network [7]. It is a binary state, irreducible, continuous-time Markov process on a static, simple, connected, undirected network $G(V, E)$. See [10, 11] for review of continuous-time Markov processes, [12, 13] for review of graph theory. Each node in the network is an agent in the population. Each node can be in one of two states, $\{0, 1\}$, representing healthy or infected state, respectively. For a network with $|V| = N$ nodes and $|E|$ edges, the state of the process at some time $t \geq 0$, which is also the microscopic network configuration, is

$$\mathbf{x} = [x_1, x_2, \ldots x_N]^T, \text{ where } x_i = \{0, 1\}.$$

As a result, there are 2^N possible configurations.

The contact process models SIS epidemics on networks. There are two types of state transitions that represent, respectively, (1) healing of infected agents and (2) infection of susceptible agents.

(1) Consider the configuration

$$\mathbf{x} = [x_1, x_2, \ldots, x_j = 1, x_{j+1}, \ldots x_N]^T.$$

Let $T_j^- \mathbf{x}$ be the configuration where the jth agent heals:

$$T_j^- \mathbf{x} = [x_1, x_2, \ldots, x_j = 0, x_{j+1}, \ldots x_N]^T.$$

The contact process transitions from $\mathbf{x}$ to $T_j^- \mathbf{x}$ in an exponentially distributed random amount of time with transition rate

$$q(\mathbf{x}, T_j^- \mathbf{x}) = \mu. \tag{1}$$

Parameter μ is the *healing rate*. Without loss of generality, we can assume $\mu = 1$.

(2) Consider the configuration

$$\mathbf{x} = [x_1, x_2, \ldots, x_{k-1}, x_k = 0, \ldots x_N]^T.$$

Let $T_k^+ \mathbf{x}$ be the configuration where the kth agent becomes infected:

$$T_k^+ \mathbf{x} = [x_1, x_2, \ldots, x_{k-1}, x_k = 1, \ldots x_N]^T.$$

The contact process transitions from $\mathbf{x}$ to $T_k^+ \mathbf{x}$ in an exponentially distributed random amount of time with transition rate

$$q(\mathbf{x}, T_k^+ \mathbf{x}) = \beta_e \sum_{i=1}^{N} x_i A_{ik}, \tag{2}$$

where $A = [A_{ik}]$ is the adjacency matrix of the underlying network. The parameter $\beta_e > 0$ is the *endogenous infection rate*. The infection rate of the kth agent is linearly dependent on its number of infected neighbours

$$m_k = \sum_{i=1}^{N} x_i A_{ik}. \tag{3}$$

The infection rate (2) assumes that the infected neighbours are independent. In the contact process, when all the agents in the network are healthy, the process dies out. The configuration where all the agents are healthy ($\mathbf{x}^0 = [0, 0, \ldots, 0]^T$) is an absorbing state of the Markov process. For networks with finite number of agents, the contact process will eventually reach the configuration $\mathbf{x}^0$ and remain there indefinitely. Thus, the equilibrium distribution is trivial for contact processes on finite-size networks [7].

2.1 *Extended contact process*

In the contact process, a healthy agent can only become infected through contagion from an infected neighbour. It may be the case that a healthy agent (or working component) may also become infected (or fail) due to an exogenous (i.e., outside of the network) source —the agent is infected spontaneously [1, 14, 15]. For SIS epidemics, this is captured by a nonzero *exogenous infection rate*, λ. The transition rate of the extended contact process from $\mathbf{x}$ to $T_k^+\mathbf{x}$ is

$$q(\mathbf{x}, T_k^+\mathbf{x}) = \lambda + \beta_e m_k, \tag{4}$$

where m_k (3) is the number of infected neighbours of agent k. The infection rate (4) assumes that the exogenous infection source and the endogenous infection sources (i.e., infected neighbours) are independent. The healing rate remains the same as (1). We call this modified model the *extended contact process*; reference [1] referred to it as the ϵ-SIS model. When agent k has 0 infected neighbours, the rate at which agent k becomes infected is the exogenous infection rate. For a system where spontaneous infection is rare, the exogenous infection rate can be made arbitrarily small, but for the extended contact process, it has to remain greater than zero.

The configuration where all the agents are healthy ($\mathbf{x}^0 = [0, 0, \ldots, 0]^T$) is no longer an absorbing state in the Markov process since susceptible agents can spontaneously become infected. As a result, the equilibrium distribution of the extended contact process is no longer trivial. There are currently no known tractable analytical results regarding this equilibrium distribution for the extended contact process for *arbitrary* network topologies; reference [1] provided analytical results when the network is a complete graph.

The equilibrium distribution can be calculated numerically. However, this approach is infeasible for large networks. In the case of an irreducible, continuous-time Markov process, the equilibrium distribution, π, is the left eigenvector of the transition rate matrix, $\mathbf{Q}_e$, corresponding to the 0 eigenvalue. However, the transition rate matrix of the extended contact process is a $2^N \times 2^N$ matrix, where N is the size of the network. Solving for the equilibrium distribution of the extended contact process over a 200-node network means finding the eigenvector of a $2^{200} \times 2^{200}$ matrix; even taking into account sparsity, such computation is clearly infeasible.

We will show in this article that we can obtain an approximation to the equilibrium distribution over arbitrary network topologies for a subset of extended contact processes using the scaled SIS process.

2.2 *Scaled SIS process*

We introduced the scaled SIS process in [8, 16]. Like the contact process, it is a binary state, irreducible, continuous-time Markov process on static, simple, connected, undirected networks. The scaled SIS process assumes that an agent can be in one of 2 states, that is, $\{0, 1\}$, representing healthy or infected state, respectively. The space of possible configurations, of the scaled SIS process is the same as that of the contact and extended contact process. The scaled SIS process also accounts for two types of state transitions representing (1) healing of infected agents and (2) infection of susceptible agents.

(1) Consider the configuration

$$\mathbf{x} = [x_1, x_2, \ldots, x_j = 1, x_{j+1}, \ldots x_N]^T.$$

Let $T_j^-\mathbf{x}$ be the configuration where the jth agent heals:

$$T_j^-\mathbf{x} = [x_1, x_2, \ldots, x_j = 0, x_{j+1}, \ldots x_N]^T.$$

The scaled SIS process transitions from $\mathbf{x}$ to $T_j^-\mathbf{x}$ in an exponentially distributed random amount of time with transition rate

$$q(\mathbf{x}, T_j^-\mathbf{x}) = \mu. \tag{5}$$

The healing rate of the scaled SIS process is the same as the healing rate of the contact process.

(2) Consider the configuration

$$\mathbf{x} = [x_1, x_2, \ldots, x_{k-1}, x_k = 0, \ldots x_N]^T.$$

Let $T_k^+\mathbf{x}$ be the configuration where the kth agent becomes infected:

$$T_k^+\mathbf{x} = [x_1, x_2, \ldots, x_{k-1}, x_k = 1, \ldots x_N]^T.$$

The scaled SIS process transitions from $\mathbf{x}$ to $T_k^+\mathbf{x}$ in an exponentially distributed random amount of time with transition rate

$$q(\mathbf{x}, T_k^+\mathbf{x}) = \lambda\beta_s^{m_k}, \tag{6}$$

where m_k is the number of infected neighbours of agent k as defined in (3). When the number of infected neighbours of agent k is 0, the infection rate is λ. Like the extended contact process, the healing and exogenous infection rates of the scaled SIS process are μ and λ respectively. Unlike the infection rate of the extended contact process (4), the infection rate of the k^{th} agent in the scaled SIS process is assumed to be *exponentially* dependent on its number of infected neighbours m_k. The parameter $\beta_s > 0$ is not the endogenous infection rate but rather the *endogenous infection factor*. The factor β_s is *not* a dimensional parameter like the endogenous infection rate β_e of the extended contact process.

We proved in [8], that, for the scaled SIS process, the resulting continuous-time Markov process is a *reversible* Markov process; a reversible Markov process is a stochastic process that is statistically the same forward in time as it is in reverse [11]. Further, we showed that the unique equilibrium distribution of the scaled SIS process over any undirected network topology described by the adjacency matrix, A, is:

$$\pi(\mathbf{x}) = \frac{1}{Z}\left(\frac{\lambda}{\mu}\right)^{1^T\mathbf{x}} \beta_s^{\frac{\mathbf{x}^T A\mathbf{x}}{2}}, \quad \mathbf{x} \in \mathscr{X}, \tag{7}$$

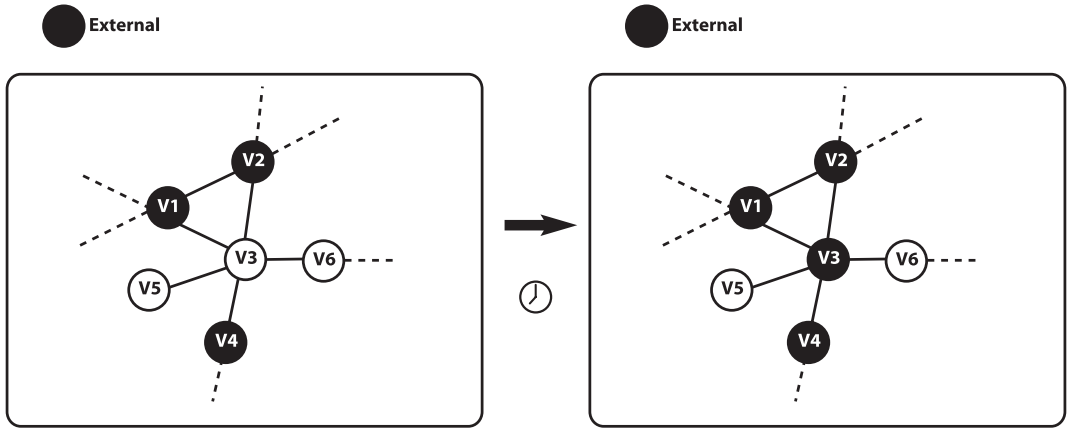

FIG. 1. Transition from configuration $\mathbf{x}$ to configuration $T_3^+\mathbf{x}$.

where 1 is the vector of all 1's, Z is the partition function, and $\mathscr{X}$ is the space of 2^N configurations. The equilibrium probability of a configuration $\mathbf{x}$ depends on the number of infected agents, $1^T\mathbf{x}$, and on the number of edges where both end nodes are infected, $\frac{\mathbf{x}^T A\mathbf{x}}{2}$.

2.3 *Extended contact process vs. scaled SIS process*

When the infection is purely exogenous (i.e, no neighbour-to-neighbour contagion), the extended contact process and the scaled SIS process are identical. The network structure does not affect the process. In this case, the process is similar to the well-known birth-death process in a finite-size population where the exogenous infection rate λ is akin to the birth rate and the healing rate μ is akin to the death rate [11].

The dynamics becomes dependent on the network when the infection rate also accounts for contagion. In both the extended contact process and the scaled SIS process, the infection rate of a susceptible agent is a function of the number of infected neighbours. However, the two models make different assumptions regarding the underlying mechanism of the contagion process:

Extended contact process

The extended contact process is parameterized by the exogenous infection rate, λ, the healing rate, μ, and the endogenous infection rate β_e. Consider the scenario in Fig. 1. Let T_3 be the random amount of time it takes for agent V_3 to become infected. Each infected neighbour of agent V_3 (i.e., V_1, V_2, V_4) and the exogenous (i.e., external) source may infect V_3 in an exponentially distributed amount of time $T_3^i \sim \exp(\beta_e), i = 1, 2, 4$, and $T_3^e \sim \exp(\lambda)$, respectively. Therefore, $T_3 = \min\{T_3^1, T_3^2, T_3^4, T_3^e\}$. Assuming that these sources act independently, then $T_3 \sim \exp(\lambda + 3\beta_e)$. As the number of infected neighbours of V_3 increases, its infection rate also increases. The extended contact process models a *distributed* contagion scenario where all the infection sources compete to be the first to infect a healthy agent.

Scaled SIS process

The scaled SIS process is parameterized by the exogenous infection rate, λ, healing rate, μ, and the endogenous factor β_s. Consider the scenario in Fig. 1. Let T_3 be the random amount of time it takes for

agent V_3 to become infected. As agent V_3 has three infected neighbours (i.e., V_1, V_2, V_4), the scaled SIS process assumes that $T_3 = \frac{1}{(\beta_s)^3} T \sim \exp(\lambda(\beta_s)^3)$, where $T \sim \exp(\lambda)$ is the random amount of time a healthy agent becomes infected when it has no infected neighbours. When $\beta_s > 1$, as the number of infected neighbours of V_3 increases, its infection rate also increases. Unlike the extended contact process, the scaled SIS process assumes an *aggregate* contagion scenario.

3. Time-asymptotic behaviour of the extended contact process

For finite-size networks, unlike the contact process, the equilibrium distribution of the extended contact process is nontrivial. In this section, we show that, for a subclass of extended contact processes over networks of *arbitrary* topology, this equilibrium distribution is well approximated by the equilibrium distribution of the scaled SIS process; for these processes, the time-asymptotic behaviour of both processes are similar.

The dynamics of a continuous-time, finite-size Markov process is summarized by its transition rate matrix $\mathbf{Q}$, where the entry $\mathbf{Q}_{i,j}$ corresponds to the transition rate of going from a Markov state i to another Markov state j. The unnormalized equilibrium distribution π of a Markov process is the left eigenvector corresponding to the 0 eigenvalue

$$\pi \mathbf{Q} = 0.$$

The non-diagonal entries of the transition rate matrix of the extended contact process, $\mathbf{Q}_e$, and the scaled SIS process, $\mathbf{Q}_s$ correspond to healing or infection rates of different individuals according to the rates (1) and (4) for the extended contact process and rates (5) and (6) for the scaled SIS process. Since there are N individuals in a network, the total number of Markov states is 2^N. Even for moderately sized networks (i.e., tens of nodes), it becomes numerical infeasible to solve for the equilibrium distribution using the eigenvalue-eigenvector approach. On the other hand, as we proved previously in [8], the equilibrium distribution of the scaled SIS process can be derived in closed-form without resorting to numerical computations. The equilibrium distribution of some extended contact processes can be approximated.

THEOREM 3.1 [Proof in Appendix 7] Consider the extended contact process with exogenous infection rate λ, healing rate μ, and endogenous infection rate β_e, over a static, simple, connected, undirected network of arbitrary topology, G. The mean and variance of the degree distribution of G are mean(d) and var(d), respectively. Let

$$\Delta = \frac{\beta_e}{\lambda}.$$

If

$$\Delta << \sqrt{\frac{2}{\text{var}(d) + (\text{mean}(d))^2 - \text{mean}(d)}},$$

then the equilibrium distribution of the extended contact process is well approximated by

$$\pi_{\text{approx}}(\mathbf{x}) = \frac{1}{Z} \left(\frac{\lambda}{\mu}\right)^{1^T \mathbf{x}} (1+\Delta)^{\frac{\mathbf{x}^T A \mathbf{x}}{2}}, \quad \mathbf{x} \in \mathscr{X}, \tag{8}$$

where A is the adjacency matrix of the network G, and Z is the partition function. The approximate distribution, $\pi_{\text{approx}}(\mathbf{x})$, is the equilibrium distribution (8) of a scaled SIS process over the same network G with exogenous infection rate λ, healing rate μ, and endogenous infection rate $\beta_s = 1 + \Delta$.

The term Δ is the ratio of the endogenous infection rate, β_e over the exogenous infection rate, λ. When $\Delta = 0$, infected neighbours are not a source of infection in the population. Consequently, this means that the infection and healing rates of the extended contact process and the scaled SIS process are identical (i.e., $\mathbf{Q}_e = \mathbf{Q}_s$). The processes would therefore have the same equilibrium distribution.

When $\Delta > 0$ but small, then $\mathbf{Q}_e \approx \mathbf{Q}_s$. In this case, the equilibrium distribution of the extended contact process and the scaled SIS process are approximately the same. Theorem 3.1 quantifies how small Δ needs to be for the approximation to hold. The approximation depends on rates and on the degree distribution of the underlying network. The distribution $\pi_{\text{approx}}(\mathbf{x})$ is a better approximate of the true equilibrium distribution of the extended contact process for networks with small average degree and/or low degree variance.

3.1 *Effects of $\frac{\lambda}{\mu}$ and $\frac{\beta_e}{\lambda}$ on the extended contact process at equilibrium*

Equation 8 shows that the approximation of the equilibrium distribution of some extended contact processes depends on the dimensionless ratios $\frac{\lambda}{\mu}$ and Δ. This section analyses how these ratios determine the dynamics.

Let $T_h \sim \exp(\mu)$ denote the random amount of time it takes for an infected agent to heal; it is equivalent to the amount of time an individual is in the infected state. Since μ is the same for all the individuals, the average amount of time to heal is the same for all infected individuals. For the extended contact process, all infection sources are *independent*. Suppose that susceptible agent i has one infected neighbour. Let $T_i^1 \sim \exp(\beta_e)$ be the random amount of time it takes for susceptible agent i to be infected by this infected neighbour, and $T_i^e \sim \exp(\lambda)$ be the random amount of time it takes for susceptible agent i to become infected by an exogenous source.

The ratio $\frac{\lambda}{\mu}$ determines the dynamics of individuals. Assuming no contagion from infected neighbours, the probability that an individual is in the healthy state *longer* than in the infected state is

$$P(T_h \leq T_i^e) = \frac{\mu}{\mu + \lambda} = \frac{1}{1 + \frac{\lambda}{\mu}}.$$

When $\frac{\lambda}{\mu} < 1$, the healing rate is faster than the exogenous infection rate. Therefore, $P(T_h \leq T_i^e) < 0.5$; this means that, on average, *assuming no endogenous contagion*, an individual spends more time in the healthy state than in the infected state. When $\frac{\lambda}{\mu} > 1$, $P(T_h \leq T_i^e) > 0.5$; it means that, on average, assuming no endogenous contagion, an individual spends more time in the infected state than in the healthy state.

The ratio $\Delta = \frac{\beta_e}{\lambda}$ compares the relative strength of endogenous infection (i.e., contagion) rate to exogenous infection (i.e, spontaneous). The probability that a susceptible agent i with one contagious neighbour is infected by the exogenous source rather than by an infected neighbour is

$$P(T_i^e \leq T_i^1) = \frac{\lambda}{\beta_e + \lambda} = \frac{1}{1 + \Delta}.$$

When $\Delta < 1$, then $P(T_i^e \leq T_i^1) > 0.5$. If a susceptible agent i has $m > 1$ contagious neighbours, the probability that agent i is infected by the exogenous source rather than by the neighbours decreases to

$$P(T_i^e \leq \min\{T_i^1, \ldots T_i^m\}) = \frac{\lambda}{m\beta_e + \lambda} = \frac{1}{1 + m\Delta}.$$

This shows that when $\Delta < 1$ and there are few infected individuals in the population, new infections are most likely due to the exogenous source. However, when there are many infected individuals in the population and the there are sufficient contacts between infected and susceptible individuals, new infections are more likely to be due to contagion.

The probability that an infected agent heals before it infects a susceptible neighbour is

$$P(T_h \leq T_i^1) = \frac{\mu}{\mu + \beta_e} = \frac{1}{1 + \frac{\beta_e}{\mu}},$$

where the ratio

$$\frac{\beta_e}{\mu} = \frac{\lambda}{\mu}\Delta.$$

When $\frac{\beta_e}{\mu} < 1$, the healing rate is faster than the endogenous infection rate. This means that the probability that an infected agent will heal before it can infect a susceptible neighbour is larger than 0.5. Whereas when $\frac{\beta_e}{\mu} > 1$ the probability that an infected agent will heal before it can infect a susceptible neighbour is less than 0.5. However, an infected agent may have many susceptible neighbours depending on the network topology.

4. Numerical experiments

We showed that the extended contact process can be well approximated by the scaled SIS process. In this section, we study Theorem 3.1 with numerical simulations. We will compare the true equilibrium distribution, $\pi_e(\mathbf{x})$, of the extended contact process, with infection and healing rates (λ, μ, β_e) over network G, with the approximation distribution, $\pi_{\text{approx}}(\mathbf{x})$. The true distribution, $\pi_e(\mathbf{x})$, is found numerically by forming the transition rate matrix, $\mathbf{Q}_e$, according to rates (1) and (4) and solving for the left eigenvector of $\mathbf{Q}_e$ corresponding to eigenvalue 0. The approximate distribution, $\pi_{\text{approx}}(\mathbf{x})$, is obtained from the closed-form equation according to Theorem 3.1

$$\pi_{\text{approx}}(\mathbf{x}) = \frac{1}{Z}\left(\frac{\lambda}{\mu}\right)^{1^T\mathbf{x}} (1+\Delta)^{\frac{\mathbf{x}^T A\mathbf{x}}{2}}, \quad \mathbf{x} \in \mathscr{X}.$$

To quantify the difference between the exact and the approximation equilibrium distribution, $\pi_e(\mathbf{x})$ and $\pi_{\text{approx}}(\mathbf{x})$, we use the total variation distance (TVD) [17]:

$$\text{TVD}(\pi_e, \pi_{\text{approx}}) = \frac{1}{2}\sum_{\mathbf{x}\in\mathscr{X}} |\pi_e(\mathbf{x}) - \pi_{\text{approx}}(\mathbf{x})|. \tag{9}$$

When the two distributions are equal, TVD is 0. The maximum TVD between any two probability distributions over the same support is 1.

As the true distribution of the extended contact process, $\pi_e(\mathbf{x})$, is obtained by solving the zero eigenvalue-eigenvector problem of $\mathbf{Q}_e$, which is a $2^N \times 2^N$ matrix, we are restricted to examples with small networks of size N.

To show numerically the goodness of the approximation, we choose to consider the six 16-node networks shown in Fig. 2 with the following structural characteristics: 1) average degree mean(d), 2) degree variance var(d), and 3) density as defined in reference [3]

$$\mathscr{D} = \frac{2|E|}{N(N-1)}. \tag{10}$$

Using the degree characteristics, we can compute for each network its limiting condition on Δ as according to Theorem 3.1,

$$\Delta_u = \sqrt{\frac{2}{\text{var}(d) + (\text{mean}(d))^2 - \text{mean}(d)}}. \tag{11}$$

Networks A and B are very structured graphs in that they have small average degree and degree variance; they are very sparse graphs and also have the largest upperbound Δ_u. Network F is also a very sparse graph but it has a large degree variance. Networks C and D are sparse and heterogeneous graphs. Network E is not a sparse graph, which by definition has $\mathscr{D} << 1$. In this respect, it is arguable that Network E is a not a realistic real-world network, which tends to be sparse. Network E has large average degree and degree variance, resulting in a small Δ_u.

In Matlab, on a Microsoft Azure cloud virtual machine with 2.6GHz Intel Xeon E5-2670 and 56GB of RAM, for a 16-node network, it takes approximately 2 s to generate the sparse transition rate matrix $\mathbf{Q}_e$ and 460 s to solve for the eigenvector corresponding to the 0 eigenvalue. For a 20-node network, it takes approximately 30 s to generate the transition rate matrix $\mathbf{Q}_e$; we receive an OUT-OF-MEMORY error when computing the eigenvector.

4.1 *Results:* $\pi_e(\mathbf{x})$ *and* $\pi_{\text{approx}}(\mathbf{x})$

When Δ is much smaller than Δ_u, the true and the approximate distributions are approximately the same. For the extended contact process with parameters $\frac{\lambda}{\mu} = 0.7, \Delta = 0.0023$, the TVD for the six networks shown in Fig. 2 are on the order of 10^{-5} to 10^{-6}. This means that the true distribution and the approximate distribution are practically identical.

Next, we consider the extended contact process with parameters $\frac{\lambda}{\mu} = 0.7, \Delta = 0.4333$, which is below Δ_u for Networks A, B, C and D and above Δ_u for Networks E and F. TVD for Networks A, B, C and D are 0.0266, 0.0290, 0.0848 and 0.1505, respectively. For Networks F, the deviation is large at 0.6652. Surprising, although $\Delta = 0.4333 > \Delta_u$ for Network E, TVD is relatively small at 0.1609. In the left columns of Figs 3 and 4, we plot the true equilibrium distribution, $\pi_e(\mathbf{x})$, of the extended contact process together with the approximate equilibrium distribution, $\pi_{\text{approx}}(\mathbf{x})$. The probability values are plotted in log scale on the Y-axis. The 2^{16} network configurations are on the X-axis. The configurations are ordered such that high probability configurations in the true distribution are in the centre. We can see highly probable configurations in the true distribution are also highly probable in the approximate distribution.

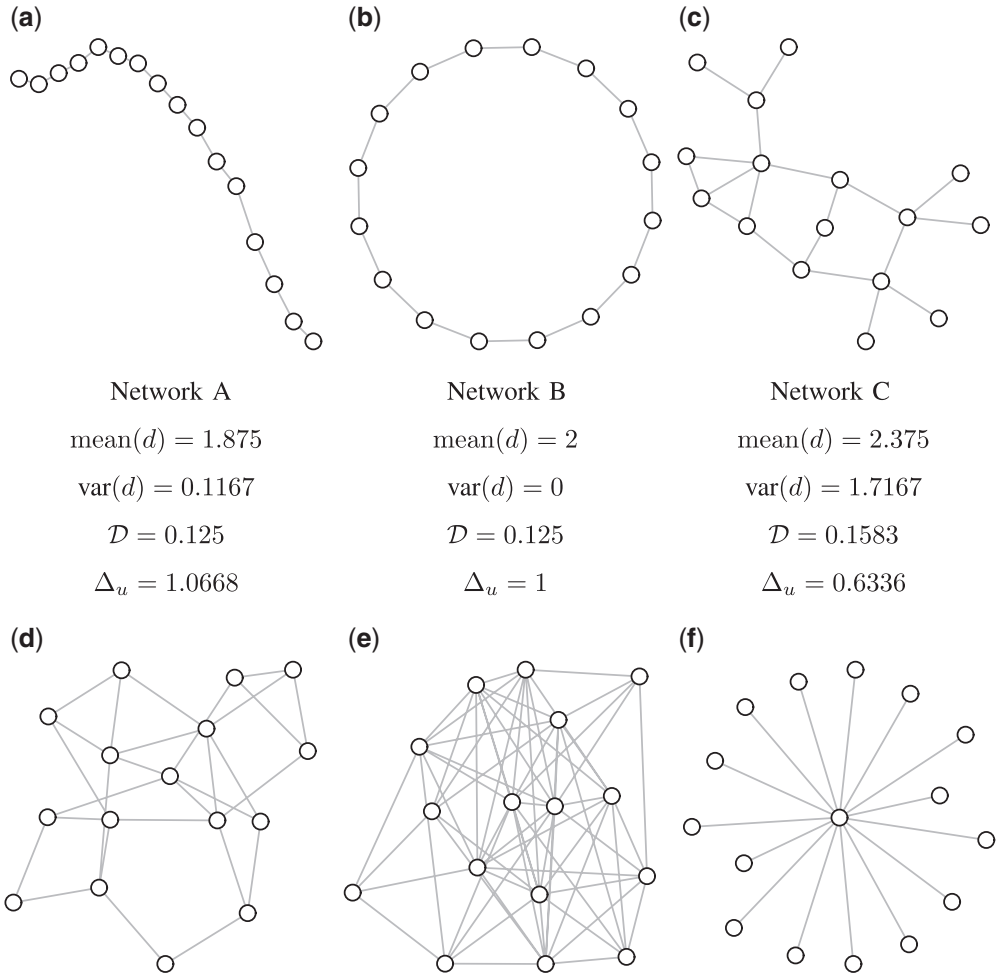

FIG. 2. Sample network topologies.

The probability that y percentage of the population is infected at equilibrium is

$$P(Y = y) = \sum_{\mathbf{x} \in \mathcal{X}: \frac{1^T \mathbf{x}}{N} = y} \pi(\mathbf{x}).$$

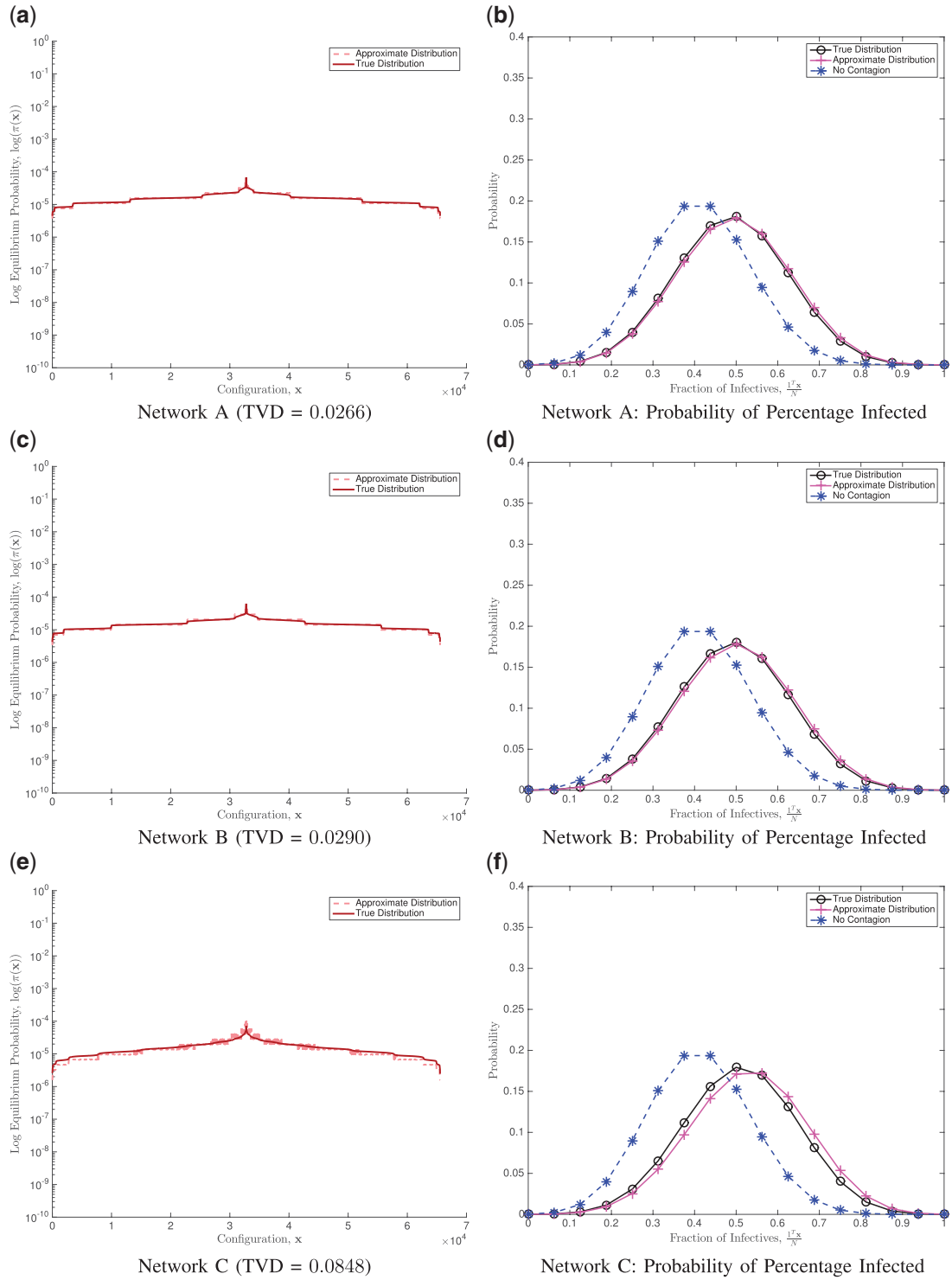

FIG. 3. $\pi_e(\mathbf{x})$ and $\pi_{approx}(\mathbf{x})$ when $\frac{\lambda}{\mu} = 0.7, \Delta = 0.4333$.

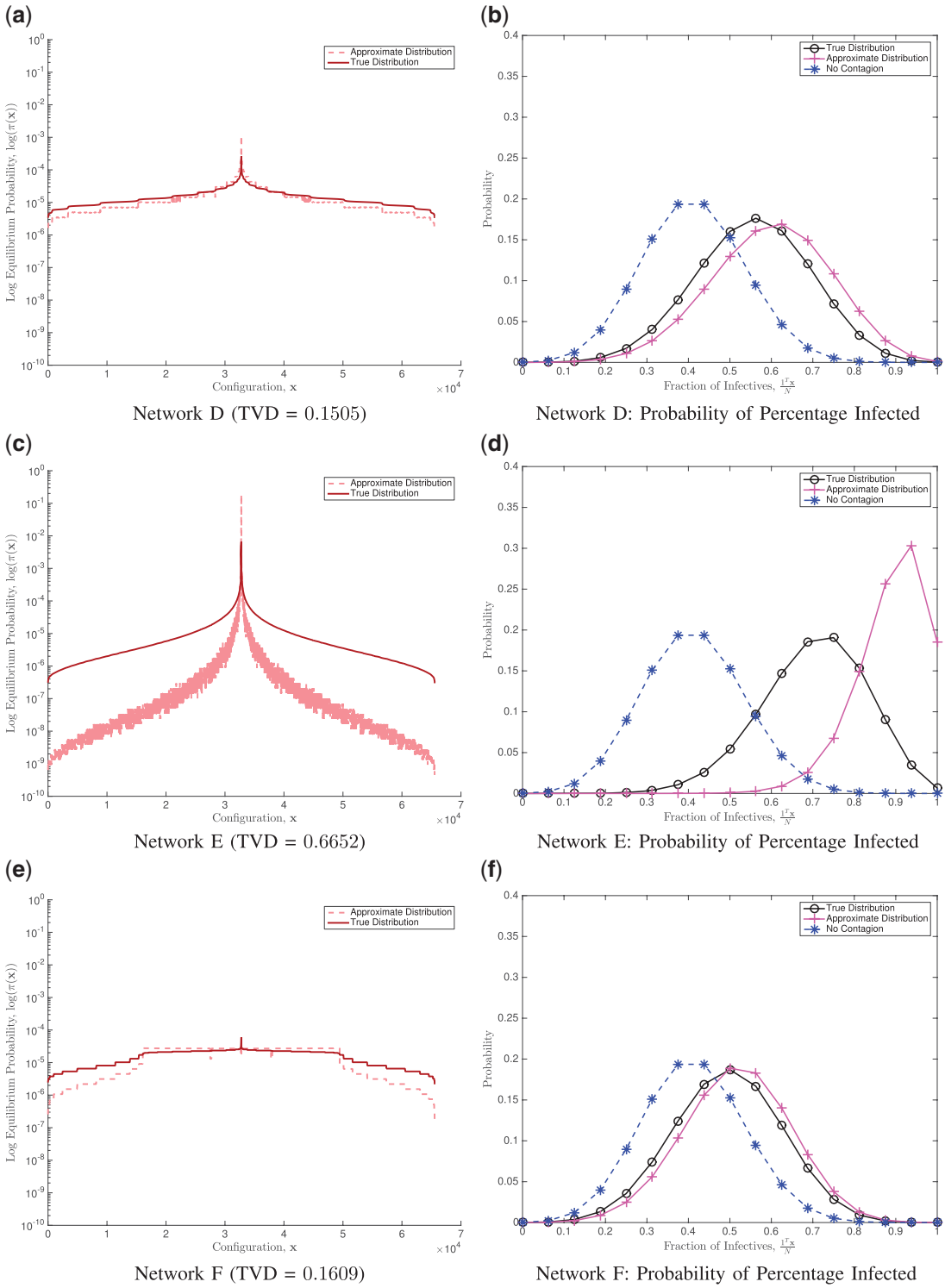

FIG. 4. $\pi_e(\mathbf{x})$ and $\pi_{approx}(\mathbf{x})$ when $\frac{\lambda}{\mu} = 0.7, \Delta = 0.4333$.

TABLE 1 *Expected percentage of infected individuals at equilibrium*

	Network A	Network B	Network C	Network D	Network E	Network F
$\mathbb{E}[Y_{\text{no contagion}}]$	0.4118	0.4118	0.4118	0.4118	0.4118	0.4118
$\mathbb{E}[Y]$	0.4888	0.4941	0.5102	0.5560	0.7029	0.4939
$\mathbb{E}[Y_{\text{approx}}]$	0.4948	0.5010	0.5289	0.5984	0.8909	0.5162

In the right columns of Figs 3 and 4, we plot $P(Y)$ for the true distribution of the extended contact process, the approximate distribution, and the case when there is no contagion from infected individual to healthy neighbours (i.e., $\beta_e = 0$). When there is no contagion, the network structure is irrelevant, and $P(Y)$ is the same for all six sample networks. The inclusion of contagion increases the probability that higher percentage of the population will be infected. When TVD is small, the distribution $P(Y)$ of the extended contact process is also well approximated by

$$P(Y_{\text{approx}} = y) = \sum_{\mathbf{x}\in\mathscr{X}:\frac{1^T\mathbf{x}}{N}=y} \pi_{\text{approx}}(\mathbf{x}).$$

We can see from Fig. 4d that when TVD is large, the fraction of infected individuals in the approximate distribution, Y_{approx}, is stochastically larger than Y. This is due to the fact that the approximate distribution, derived from the scaled SIS process, has higher infection rate than the extended contact process. Table 1 shows the expected percentage of infected individuals for all three distributions. We can see that

$$\mathbb{E}[Y_{\text{no contagion}}] \leq \mathbb{E}[Y] \leq \mathbb{E}[Y_{\text{approx}}].$$

4.2 *Results: TVD vs.* Δ *and* $\frac{\lambda}{\mu}$

The approximate equilibrium distribution of the extended contact process depends on $\frac{\lambda}{\mu}$, the ratio of exogenous infection rate and the healing rate, and Δ, the ratio of the endogenous infection rate and the exogenous infection rate. We study here the dependence of the approximation of $\pi_e(\mathbf{x})$ by $\pi_{\text{approx}}(\mathbf{x})$ on $\frac{\lambda}{\mu}$ and Δ. In Fig. 5, we plot Δ along the X-axis and the TVD between $\pi_e(\mathbf{x})$ and $\pi_{\text{approx}}(\mathbf{x})$ along the Y-axis for the six network topologies shown in Fig. 2. Different curves in each figure correspond to equilibrium distributions with different $\frac{\lambda}{\mu}$ values.

As expected, when $\Delta << \Delta_u$ for all six topologies, TVD is negligible for all the networks. Deviation between the true equilibrium distribution and the approximation increases as Δ moves toward Δ_u. Since Δ_u depends on the mean and variance of the degree distribution, the rate of increase of TVD as Δ increases from 0 also depends on the mean and variance of the degree. Surprisingly, this increase is *not* monotonic for *all* network topologies. As Δ increases to values larger than Δ_u, TVD may decrease. We observe this decrease in TVD for both Network E in Fig. 5e and Network F in Fig. 5f. These networks have large degree variance; this means that some nodes have much larger degree than others. At larger Δ, these highly connected nodes increase the probability of configurations with large numbers of infected individuals, thereby decreasing the deviation between the true distribution and the approximate distribution.

From these studies, we conclude that the equilibrium distribution of the extended contact process can be well approximated by $\pi_{\text{approx}}(\mathbf{x})$ when the condition in Theorem 3.1 is satisfied. We will use this result in Section 6 where we study the equilibrium distribution for the extended contact process on a much larger real-world network—the 4941-node US Western power grid [18].

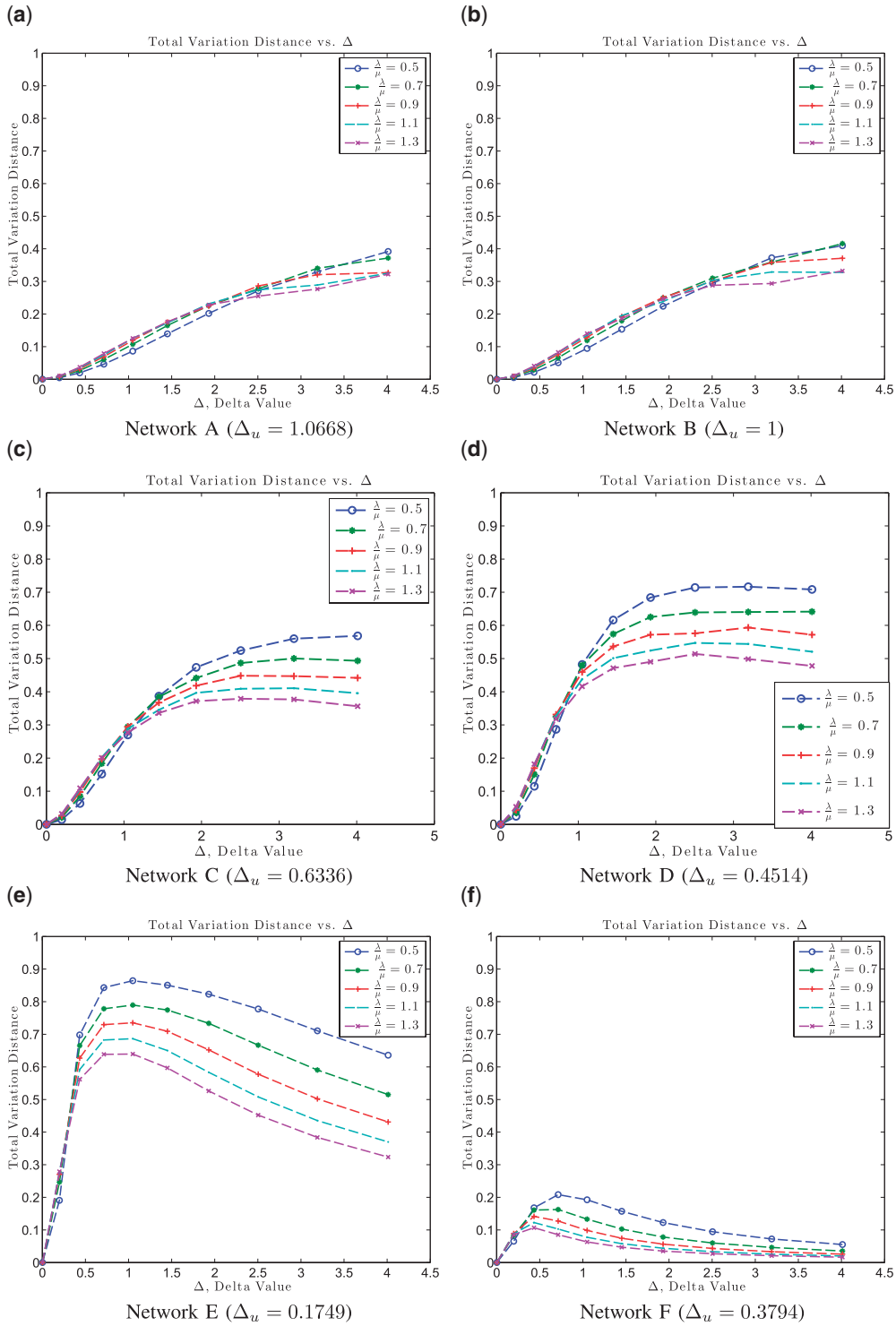

FIG. 5. Dependence of TVD($\pi_e, \pi_{\text{approx}}$) on Δ.

5. Most-probable configuration

We showed in Figs 3 and 4 that, for a range of the dynamic parameters, the equilibrium distribution $\pi_e(\mathbf{x})$ of the extended contact process is well approximated by the equilibrium distribution $\pi_{\text{approx}}(\mathbf{x})$ of the scaled SIS process. In this section, we study the more detailed question of finding the most-probable configuration (i.e., the configuration with the maximum equilibrium probability). We consider the small networks of Section 4 so that we can compare the true most-probable configuration with the maximizer of the approximation distribution. In Section 6, we apply the approximation to solve for the most-probable configuration of a large real-world network.

For network processes, the most-probable configuration depends on the infection and healing rates and on the underlying network topology. It identifies the set of agents that are most likely to be infected in the long run. These are the more vulnerable agents in the network. If the most probable configuration is $\mathbf{x}^0 = [0, 0, \ldots 0]^T$, all agents are healthy, whereas if the most-probable configuration is $\mathbf{x}^N = [1, 1, \ldots 1]^T$, then all agents are at risk regardless of their location in the network. Except for these two cases, finding which agents are infected in the most-probable configuration is not trivial. The most-probable configuration of the extended contact process is

$$\mathbf{x}_e^* = \arg\max_{\mathbf{x}\in\mathscr{X}} \pi_e(\mathbf{x}).$$

For the extended contact process, there is no closed-form description of the equilibrium distribution, so this problem can only be solved numerically, which is infeasible for large-scale networks.

On the other hand, as stated in Theorem 3.1, when $\Delta << \Delta_u$, the equilibrium distribution, $\pi_e(\mathbf{x})$, of the extended contact process is well approximated by the equilibrium distribution, $\pi_{\text{approx}}(\mathbf{x})$, of a scaled SIS process with endogenous infection rate $\beta_s = 1 + \Delta$. We proved in [9] that, in this case, the most-probable configuration of the scaled SIS process can be solved in *polynomial-time* because it corresponds to solving for the minimum of a submodular function. It is therefore possible to identify vulnerable network substructures for networks with hundreds and thousands of agents using $\pi_{\text{approx}}(\mathbf{x})$.

From the simulation results in the previous section, we now compare the most-probable configuration of the extended contact process with the most-probable configuration found with the approximating scaled SIS process. Table 2 lists for the six networks in Fig. 2, the TVD between the distributions, the corresponding most-probable configurations, and the probabilities of the most-probable configuration for $\frac{\lambda}{\mu} = 0.9744$ and $\Delta = 0.02$. We observe that when Δ is very small:

TABLE 2 *Most-probable configuration when* $\frac{\lambda}{\mu} = 0.9744$ *and* $\Delta = 0.02$

	$\text{TVD}(\pi_e, \pi_{\text{approx}})$	$\mathbf{x}_e^*$	$\mathbf{x}_{\text{approx}}^*$	$\pi_e(\mathbf{x}_e^*)$	$\pi_{\text{approx}}(\mathbf{x}_{\text{approx}}^*)$
Network A	1.0236×10^{-4}	$\mathbf{x}^0 = [0, 0, \ldots 0]^T$	$\mathbf{x}^0 = [0, 0, \ldots 0]^T$	1.7431×10^{-5}	1.7427×10^{-5}
Network B	1.1027×10^{-4}	$\mathbf{x}^0 = [0, 0, \ldots 0]^T$	$\mathbf{x}^0 = [0, 0, \ldots 0]^T$	1.7347×10^{-5}	1.7342×10^{-5}
Network C	3.3806×10^{-4}	see Fig. 6c	see Fig. 6c	1.7107×10^{-5}	1.7154×10^{-5}
Network D	5.2714×10^{-4}	$\mathbf{x}^N = [1, 1, \ldots 1]^T$	$\mathbf{x}^N = [1, 1, \ldots 1]^T$	1.8622×10^{-5}	1.8781×10^{-5}
Network E	0.0031	$\mathbf{x}^N = [1, 1, \ldots 1]^T$	$\mathbf{x}^N = [1, 1, \ldots 1]^T$	3.1073×10^{-5}	3.277×10^{-5}
Network F	0.0023	$\mathbf{x}^0 = [0, 0, \ldots 0]^T$	$\mathbf{x}^0 = [0, 0, \ldots 0]^T$	1.7419×10^{-5}	1.7389×10^{-5}

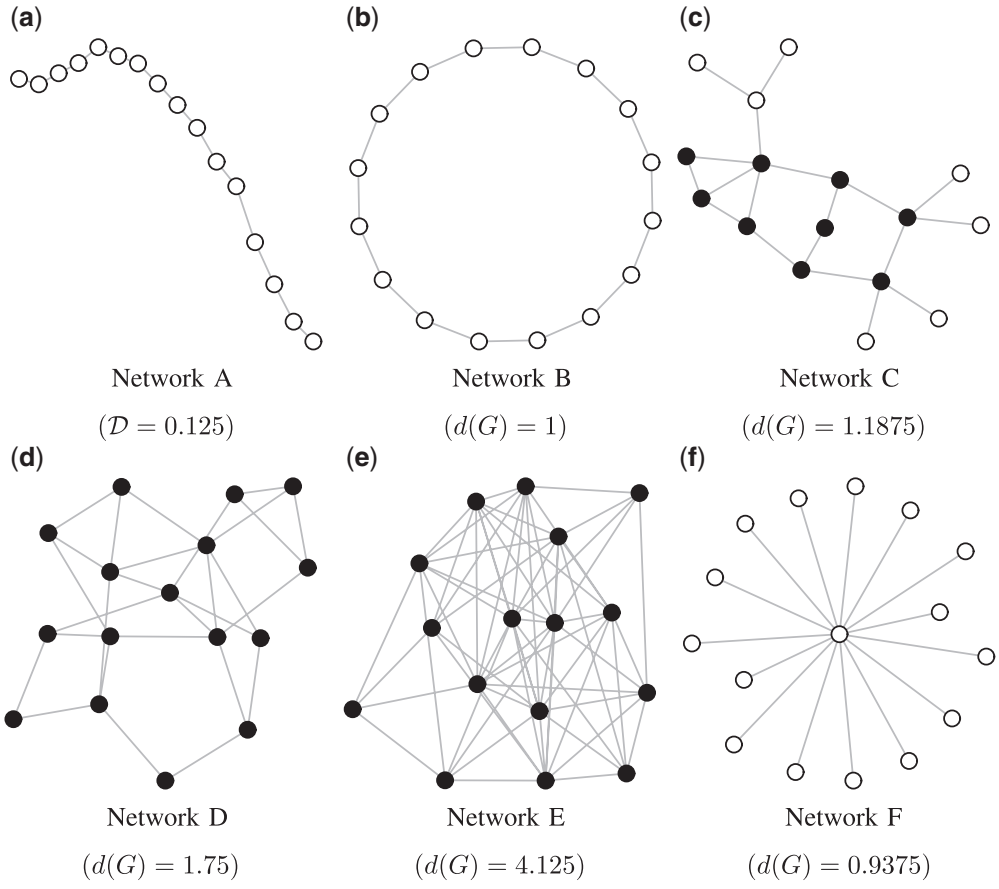

FIG. 6. Most probable configuration when $\frac{\lambda}{\mu} = 0.9744$ and $\Delta = 0.02$ (infected = black, healthy = white).

(1) the most-probable configuration, $\mathbf{x}_e^*$, of the extended contact process is the same as the most-probable configuration, $\mathbf{x}_{\text{approx}}^*$, of the scaled SIS process;

(2) the probability of the most-probable configuration, $\pi_e(\mathbf{x}_e^*)$, of the extended contact process is approximately the same as the probability of the most-probable configuration, $\pi_{\text{approx}}(\mathbf{x}_{\text{approx}}^*)$, of the scaled SIS process.

For Networks A, B and F, the most-probable configuration for both the extended contact process and the approximate scaled SIS process is $\mathbf{x}^0$, the configuration where all the agents are healthy. However, for the same infection and healing rate, the most-probable configuration for Networks D and E for both the extended contact process and the scaled SIS process is $\mathbf{x}^N$, the configuration where all the agents are infected. Figure 6c shows that the most-probable configuration for Network C is neither $\mathbf{x}^0$ nor $\mathbf{x}^N$ but a configuration where nine agents are infected while seven agents are healthy; we call most-probable configurations that are neither $\mathbf{x}^0$ nor $\mathbf{x}^N$ *non-degenerate* most-probable configurations.

TABLE 3 *Most-probable configuration when* $\frac{\lambda}{\mu} = 0.7$ *and* $\Delta = 0.4333$

	$\text{TVD}(\pi_e, \pi_{\text{approx}})$	$\mathbf{x}_e^*$	$\mathbf{x}_{\text{approx}}^*$	$\pi_e(\mathbf{x}_e^*)$	$\pi_{\text{approx}}(\mathbf{x}_{\text{approx}}^*)$
Network A	0.0266	$\mathbf{x}^0 = [0, 0, \ldots 0]^T$	$\mathbf{x}^0 = [0, 0, \ldots 0]^T$	6.7989×10^{-5}	6.4085×10^{-5}
Network B	0.029	$\mathbf{x}^0 = [0, 0, \ldots 0]^T$	$\mathbf{x}^N = [1, 1, \ldots 1]^T$	6.2942×10^{-5}	6.1972×10^{-5}
Network C	0.0848	see Fig. 6c	$\mathbf{x}^N = [1, 1, \ldots 1]^T$	7.0847×10^{-5}	1.214×10^{-4}
Network D	0.1505	$\mathbf{x}^N = [1, 1, \ldots 1]^T$	$\mathbf{x}^N = [1, 1, \ldots 1]^T$	2.5957×10^{-4}	0.0011
Network E	0.6652	$\mathbf{x}^N = [1, 1, \ldots 1]^T$	$\mathbf{x}^N = [1, 1, \ldots 1]^T$	0.0066	0.1849
Network F	0.1609	$\mathbf{x}^0 = [0, 0, \ldots 0]^T$	$\mathbf{x}^N = [0, 0, \ldots 0]^T$	5.988×10^{-5}	3.7915×10^{-5}

For an extended contact process with exogenous infection rate and healing rate, $\frac{\lambda}{\mu} = 0.9744$, and endogenous infection rate, $\Delta = 0.02$, the epidemic is minor in Networks A, B and F, but should be of concern in Networks D and E. In Network C, a subset of agents are more at risk than others. Different networks have different risk levels because the propagation of contagious infection is dependent on the underlying network topology. The result in Fig. 6c confirms for the extended contact process what we had proved for the scaled SIS process in [9], namely that, in the most-probable configuration, infected agents belong to dense subgraphs in the network.

Networks with high density, such as Networks D and E are more at risk to contagion than networks with low density such as Networks A, B and F. Network F, although it has the largest maximum degree, has the same density as Network A. It is difficult for infection to spread in Network F because the centre agent is the only agent capable of transmitting the infection to its neighbours. We showed in [9] that the nine infected agents in Network C are more at risk of infection than the other agents because they form a subgraph that is denser than the overall network. Using the definition of density in (10), the density of the subgraph induced by these nine individuals is 0.333 compared with the density of the overall network, which is 0.1583; these nine agents are especially well connected and are therefore more prone to contagion.

Table 3 lists the TVD between the distributions, the most-probable configurations for the extended contact process and the approximate scaled SIS process, and the probabilities of the most-probable configurations for $\frac{\lambda}{\mu} = 0.7$ and $\Delta = 0.4333$. As Δ is larger, the most-probable configurations may not be the same in the true and approximation distributions, as for Networks B and C, even though the probabilities of the most-probable configurations are similar. Alternatively as for Networks D and E, $\mathbf{x}_e^*$ and $\mathbf{x}_{\text{approx}}^*$ are identical but the corresponding probabilities are magnitudes apart.

Note that the configuration in Fig. 6c, where nine agents are more at risk of infection than others, remains the most-probable configuration for Network C. Even though this configuration no longer has the highest equilibrium probability in the approximate distribution, it remains a highly probable configuration. This reinforces our observation from Figs 3 and 4 that configurations with high probabilities in the approximate distribution are also highly probable in the equilibrium distribution of the extended contact process. The substructures that are vulnerable for the scaled SIS process, the *non-degenerate* most-probable configurations, are also vulnerable substructures of the extended contact process.

6. Real-world network

Real-world networks are often much larger than 16 nodes. Assuming that exogenous infection corresponds to spontaneous component failure, endogenous infection corresponds to cascading failure, and healing

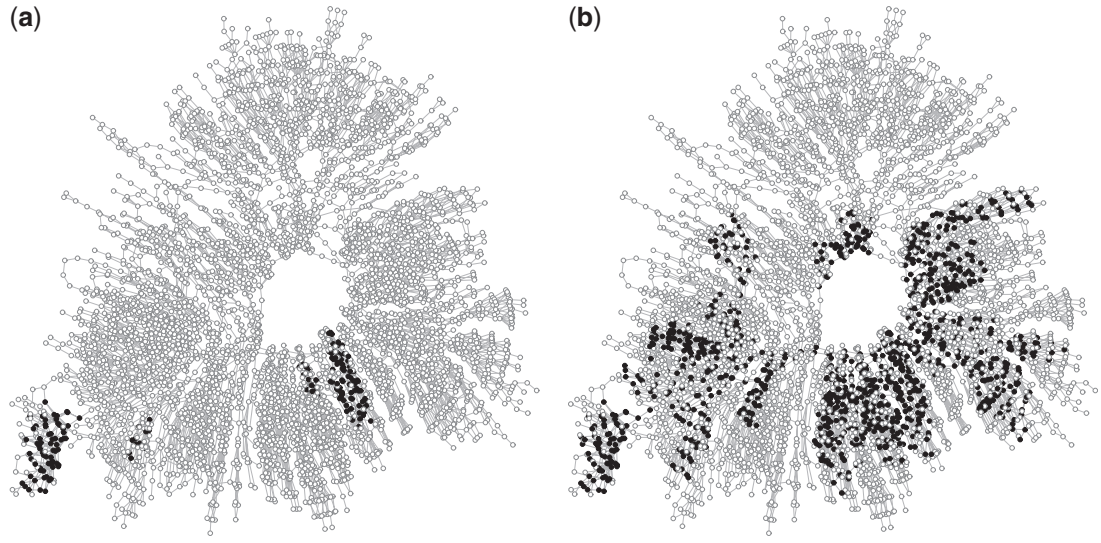

FIG. 7. US Western power grid $\mathbf{x}^*$ (infected = black and healthy = white) mean(d) = 2.6691 var(d) = 3.2093 $\mathscr{D}$ = 0.00054 $\Delta_u = 0.5108$.

to recovery, we use the extended contact process to model blackout processes in the power grid. We use the 4941-node network representation of the US Western power grid [18]. It is a sparse, heterogeneous network. Its size precludes the numerical computation of the equilibrium distribution of the extended contact process; the transition rate matrix is a $2^{4941} \times 2^{4941}$ matrix. In this section, we use Theorem 3.1 to approximate $\pi_e(\mathbf{x})$ by the closed-form equilibrium distribution $\pi_{\text{approx}}(\mathbf{x})$ when $\Delta < \Delta_u = 0.5108$. Figure 7a and b shows the most-probable configurations computed from the approximate equilibrium distribution for the extended contact process with parameters $\frac{\lambda}{\mu} = 0.6, \Delta = 0.3$ and $\frac{\lambda}{\mu} = 0.8888$, $\Delta = 0.08$. This computation can be done efficiently (i.e., less than 1 s on a standard desktop) [19]. These configurations are non-degenerate and show the subsets of components (black coloured nodes) that are more vulnerable to failures than other subsets (white coloured nodes).

7. Conclusion

This article derived a condition under which the equilibrium distribution of the extended contact process [1, 15] is well approximated by the equilibrium distribution of a scaled SIS process [8]. The two processes are similar when $\frac{\beta_e}{\lambda} << \Delta_u$. The condition Δ_u is larger when the underlying network is sparsely connected with small degree variance than when the network is densely connected. With the closed-form approximate equilibrium distribution, we can study the behaviour of the extended contact process on networks with thousands of nodes whereas we can only calculate the equilibrium distribution of the extended contact process using numerical methods for networks with tens of nodes.

We show that the equilibrium behaviour of a subclass of extended contact processes depends on two parameter ratios: $\frac{\lambda}{\mu}$ and Δ and two statistics: the number of infected nodes and the number of edges where both end nodes can be infected. Further, using the closed-form approximation to the equilibrium

distribution, we can solve for the most-probable configuration in polynomial-time. This shows which subset of nodes in the network may be more vulnerable than other subsets. The more vulnerable nodes are reflected by the non-degenerate solutions of the most-probable configuration problem. As we discussed in [9], non-degenerate solutions arise due to the existence of subgraphs in the network with higher densities than the overall network. Our method not only proves that more densely connected communities are more vulnerable to contagion, but also gives a polynomial-time method to identify such communities.

Acknowledgements

We thank Microsoft for providing us their cloud computational resources with a Microsoft Azure Research Award. We also thank the two anonymous reviewers for their insightful comments, which contributed significantly to the manuscript.

Funding

This work is partially supported by AFOSR grant FA95501010291 and by NSF grants CCF1011903 and CCF1513936.

References

1. Van Mieghem, P. & Cator, E. (2012) Epidemics in networks with nodal self-infection and the epidemic threshold. *Phys. Rev. E*, **86**, 016116.
2. Diekmann, O., Heesterbeek, H. & Britton, T. (2012) *Mathematical Tools for Understanding Infectious Disease Dynamics*. Princeton, New Jersey: Princeton University Press.
3. Barrat, A., Barthelemy, M. & Vespignani, A. (2008) *Dynamical Processes on Complex Networks*. Cambridge, England: Cambridge University Press.
4. Keeling, M. J. & Eames, K. T. (2005) Networks and epidemic models. *J. R. Soc. Interface*, **2**, 295–307.
5. Porter, M. A. & Gleeson, J. P. (2014) Dynamical systems on networks: A tutorial. *arXiv preprint arXiv:1403.7663*.
6. Pellis, L., Ball, F., Bansal, S., Eames, K., House, T., Isham, V. & Trapman, P. (2014) "Eight challenges for network epidemic models," *Epidemics*, **10**, 58–62.
7. Liggett, T. M. (1999) *Stochastic Interacting Systems: Contact, Voter and Exclusion Processes*, vol. 324. Berlin, Germany: Springer.
8. Zhang, J. & Moura, J. M. F. (2014) "Diffusion in social networks as SIS epidemics: Beyond full mixing and complete graphs," *IEEE J. Sel. Topics Signal Process.*, **8**, pp. 537–551.
9. Zhang, J. & Moura, J. M. F. (2015) "Role of subgraphs in epidemics over finite-size networks under the scaled SIS process," *J. Complex Networks*, **3**, 584–605.
10. Norris, J. R. (1998) *Markov Chains*. Cambridge, England: Cambridge University Press.
11. Kelly, F. P. (2011) *Reversibility and Stochastic Networks*. Cambridge, England: Cambridge University Press.
12. West, D. B. (2001) *Introduction to Graph Theory* vol. 2. Upper Saddle River, New Jersey: Prentice hall Upper Saddle River.
13. Godsil, G. R. C. (2001) *Algebraic Graph Theory*. Berlin, Germany: Springer.
14. Santos, A. & Moura, J. M. F. (2011) Emergent behavior in large scale networks. *2011 50th IEEE Conference on Decision and Control and European Control Conference (CDC-ECC)*. IEEE, pp. 4485–4490.
15. Zhang, J. & Moura, J. M. F. (2012) Accounting for topology in spreading contagion in non-complete networks. *2012 IEEE International Conference on Acoustics, Speech and Signal Processing (ICASSP)*. pp. 2681–2684.
16. Zhang, J. & Moura, J. M. F. (2013) Threshold behavior of epidemics in regular networks. *2013 IEEE International Conference on Acoustics, Speech and Signal Processing (ICASSP)*, pp. 5411–5414.

17. LEVIN, D. A., PERES, Y. & WILMER, E. L. (2009) *Markov Chains and Mixing Times*. Providence, RI: American Mathematical Soc.
18. LESKOVEC, J. & KREVL, A. (2014) SNAP Datasets: Stanford large network dataset collection. http://snap.stanford.edu/data (lase accessed on 8 March 2017).
19. ZHANG, J. (2015) Network process: How topology impacts the dynamics of epidemics and cascading failures. *Ph.D. Dissertation*, Pittsburgh, PA, USA: Carnegie Mellon University.

Appendix. Proof of Theorem 3.1

THEOREM Consider the extended contact process with exogenous infection rate λ, healing rate μ, and endogenous infection rate β_e, over a static, simple, connected, undirected network of arbitrary topology, G. The mean and variance of the degree distribution of G are mean(d) and var(d), respectively. Let

$$\Delta = \frac{\beta_e}{\lambda}.$$

If

$$\Delta << \sqrt{\frac{2}{\text{var}(d) + (\text{mean}(d))^2 - \text{mean}(d)}},$$

then the equilibrium distribution of the extended contact process is well approximated by

$$\pi_{\text{approx}}(\mathbf{x}) = \frac{1}{Z}\left(\frac{\lambda}{\mu}\right)^{1^T\mathbf{x}}(1+\Delta)^{\frac{\mathbf{x}^T A\mathbf{x}}{2}}, \quad \mathbf{x} \in \mathscr{X},$$

where A is the adjacency matrix of the network G, and Z is the partition function. The approximate distribution, $\pi_{\text{approx}}(\mathbf{x})$, is the equilibrium distribution (8) of a scaled SIS process over the same network G with exogenous infection rate λ, healing rate μ, and endogenous infection rate $\beta_s = 1 + \Delta$.

Proof. From the theory of continuous-time Markov processes [10], the equilibrium distribution of the extended contact process is the left eigenvector of the transition rate matrix, $\mathbf{Q}_e$, corresponding to the 0 eigenvalue:

$$\pi\mathbf{Q}_e = 0.$$

Entries of the transition rate matrix of the extended contact process, $\mathbf{Q}_e$, correspond to the transition rates from one Markov state to another according to the rates (1) and (4) depending on parameters λ, β_e, μ. Entries of the transition rate matrix of the scaled SIS process, $\mathbf{Q}_s$, correspond to the transition rates from one Markov state to another according to the rates (5) and (6) depending on parameters λ, β_s, μ. Consequently, the only entries that may differ between $\mathbf{Q}_e$ and $\mathbf{Q}_s$ correspond to the infection rates.

Let

$$\Delta = \frac{\beta_e}{\lambda}.$$

When $\Delta = 0$, there is no contagion from infected agent to susceptible neighbour. As a result, $\mathbf{Q}_e = \mathbf{Q}_s$. When $\Delta << 1$, then $\mathbf{Q}_e \approx \mathbf{Q}_s$. We can derive a more insightful condition on Δ that depends on the underlying network structure.

Consider a susceptible agent with m infected neighbours. Then the Taylor series expansion of the infection rate of the susceptible agent under the dynamics of the scaled SIS process with parameters $\lambda, \beta_s = 1 + \Delta, \mu$ is

$$\lambda \beta_s^m = \lambda(1 + \Delta)^m \approx \lambda + \lambda \Delta m + \text{higher order terms}.$$

The linear term of the Taylor series expansion is the infection rate of the extended contact process, with parameters λ, β_e, μ. When $m = 0$, then $\mathbf{Q}_e = \mathbf{Q}_s$. Otherwise, for $\mathbf{Q}_e \approx \mathbf{Q}_s$, the higher order terms must be negligible. This means that the quadratic term

$$\frac{m(m-1)}{2}\Delta^2 << 1.$$

Where all neighbours of the susceptible agent are infected, m is the nodal degree. Therefore the worst case scenario, in the sense that $\mathbf{Q}_e$ and $\mathbf{Q}_s$ have the largest deviation, is dependent on the maximum nodal degree, $d_{\max}$, of the underlying network. The most restrictive condition on Δ is

$$\frac{d_{\max}(d_{\max}-1)}{2}\Delta^2 << 1.$$

However, instead of working with the worst case scenario, we considered the case where

$$\mathbb{E}\left[\frac{m(m-1)}{2}\right]\Delta^2 << 1.$$

As a result, we derived the following, less restrictive, condition on Δ,

$$\Delta << \sqrt{\frac{2}{\text{var}(d) + (\text{mean}(d))^2 - \text{mean}(d)}},$$

where $\text{mean}(d)$ and $\text{var}(d)$ are the mean and variance of the degree distribution. Since the infection rates are similar for the extended contact process and the scaled SIS process, then $\mathbf{Q}_e \approx \mathbf{Q}_s$. Therefore, the equilibrium distribution of the extended contact process with parameters λ, β_e, μ, can be approximated by the equilibrium distribution of the scaled SIS process with parameters $\lambda, \beta_s = 1 + \Delta, \mu$, which we derived in [8] to be

$$\pi_{\text{approx}}(\mathbf{x}) = \frac{1}{Z}\left(\frac{\lambda}{\mu}\right)^{1^T\mathbf{x}}(1+\Delta)^{\frac{\mathbf{x}^T A\mathbf{x}}{2}}, \quad \mathbf{x} \in \mathscr{X}. \qquad \square$$